UNIVERSITY OF WEST BOHEMIA

Applied and Computational Mechanics 2 (2008) 323–334

Applied and Computational Mechanics

The influence of the excitation pulse shape on the stress wave propagation in a bcc iron crystal

V. Pelikán[a,*], P. Hora[a], A. Machová[b], O. Červená[a]

[a] *Institute of Thermomechanics of the ASCR, v.v.i., Veleslavínova 11, 301 14 Plzeň, Czech Republic*
[b] *Institute of Thermomechanics of the ASCR, v.v.i., Dolejškova 5, 182 00 Praha, Czech Republic*

Received 26 August 2008; received in revised form 24 October 2008

Abstract

This article presents a large-scale molecular dynamic simulations of wave propagation in a cracked bcc (body centered cubic) iron crystal based on an N-body potential model which gives a good description of an anisotropic elasticity. The crystal is loaded by a stress pulse on its front face and the response is detected on its opposite face. The various shapes, amplitudes, and widths of stress pulse are considered. The simulations are performed also for a central pre-existing Griffith crack. The crack is embedded in a bcc iron crystal having a basic cubic orientation. The acquired results bring important information for further analysis oriented to new NDT nanoscale methods.

Keywords: molecular dynamics, bcc iron crystal, wave propagation

1. Introduction

There is an increasing interest in molecular dynamic (MD) simulations (e.g. [1, 4, 5, 6]) since they can bring valuable information on micromechanics and kinetics of failure in materials, which is often not accessible for experiments. Moreover, MD simulations use an independent failure criterion (cut-off radius of nonlinear interatomic forces) and thus, they can verify continuum predictions both in linear and nonlinear region of loading.

Our work is motivated by efforts to recognize (to "see") a pre-existing crack of nano-scale dimensions by means of elastic wave propagation in body centered cubic (bcc) atomic lattice of iron. The studies utilize scattering of the elastic stress waves and nonlinear effects. The crystal is loaded by a pressure pulse from an external sample surface. The mechanical response to interior defect is monitored on the both external and front free sample surfaces via a map of the atomic displacements and velocities. The results will be compared with the dynamic response in perfect crystals. We believe that this research can bring useful new information for nondestructive testing (NDT) on nano scale level.

We utilize 3D atomistic simulations by molecular dynamic technique with an N-body potential for bcc iron [2] of Finnis-Sinclair type [3] and parallel programming [7]. Present work is a continuation of the studies published in [8, 9, 10]. The behavior of stress waves caused by a surface impulsion in perfect crystals is described in [8, 9]. The N-body potential gives a good description of an anisotropic elasticity. The mechanical response of the crack to point, line and surface impulsions of Heaviside type is studied in [10]. The latest study shows that the most

*Corresponding author. Tel.: +420 377 236 415, e-mail: pelikan@cdm.it.cas.cz.

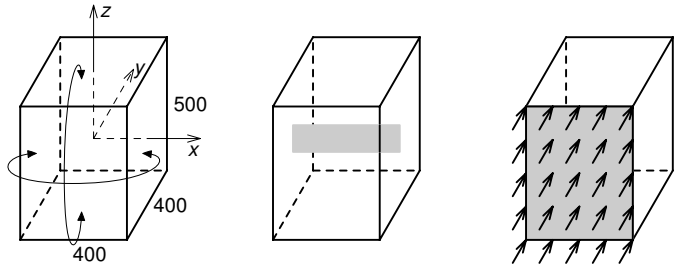

Fig. 1. The geometry of used sample, the crack location, and type of loading

effective way how to detect the crack in the framework of the non-linear atomistic model is the surface excitation.

In present simulations the stress wave propagation is studied both in perfect crystal and in the presence of a crack. A central Griffith crack is embedded in a bcc iron crystal with the basic cubic orientation. The crystal is loaded by a surface stress pulse on its front face and the response is detected on its opposite face and also on the front face. The various shapes, amplitudes, and widths of a stress pulse are considered. The tasks of this type have a physical sense only if the information is not influenced by the stress wave reflections from the free surfaces of the atomistic samples. For that reason the samples should be large enough and the simulations on these models can be realized only with a massive application of parallel programming techniques, [7].

2. Description of numerical MD experiments

All MD simulations were performed on a bcc iron plates with the lattice constant $a_0 = 2.8665\,\text{Å}$. The plate thickness was 400 atoms in the y axis direction. The infinity in the other two directions was reached by the application of the periodic boundary conditions on the rectangular sample with the edge of 400 atoms in the x axis direction and the edge of 500 atoms in the z axis direction (fig. 1 – left). The pre-existing Griffith crack is created in the middle of the crystal (fig. 1 – center) by removing 3 atomic $\{100\}$ layers, i.e. the initial crack thickness corresponds to $2a_0$ and its width is $100\,a_0$. Since the Fe–Fe potential from [2] is short ranged (cut-off radius is 1.3 a_0), interatomic interactions between the free crack faces do not exist initially. This can be changed when a pressure pulse reaches the crack faces. The sample without a crack contains totally 159 800 000 atoms. The sample with the crack contains totally 159 680 400 atoms. The all-area excitation in the y axis direction on the front side has been used as a loading (fig. 1 – right). Surface relaxation has been performed in the sample before external loading. Initial temperature corresponded to 0 K and further thermal atomic motion was not controlled in the system. Loading is applied in the y-direction by applying external forces $F_{ext} = \sigma_A a_0^2$ on each atom in the first surface layer. The applied stress σ_A has two pulse shapes with a various width and amplitude. The stress pulses began at 30^{th} time integration step. The pulse shapes, their widths and the values of applied stress in GPa are given in tab. 1. The performed simulations for particular shapes and widths of pulses, and for individual levels of loading are marked (✓) in this table. The denoted simulations were done both for the sample without a crack and for the sample with the Griffith crack. All tests, where the local atomic interactions across the free crack faces were monitored, are marked by the star (*). The tests denoted by circled number are used in the following chapter.

Table 1. The excitation pulse types

Stress pulse shape	Pulse width [fs]	Applied stress		
		Level 1 0.675 GPa	Level 2 2.700 GPa	Level 3 10.800 GPa
	200	✓	✓	✓ ①
	400		✓	✓* ②
	800		✓ ③	
	1 600		✓* ④	
	400			✓
	800			✓
	1 600		✓	✓* ⑤

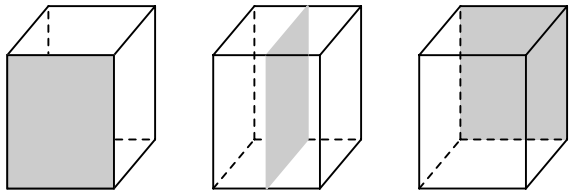

Fig. 2. The atom location selected for an output file

To solve Newtonian equations of motion we used a time integration step 10^{-14} s in all simulations. The tests were done between the steps 0 and 3 000. The total energy balance (the kinetic energy, the potential energy and the work of external forces), the total number of the atomic interactions, and the local number of the atomic interactions at free crack faces were monitored at each time step. The total number of the interactions for the sample without a crack was constant (1 117 400 000), and for the sample with the crack was either constant (1 116 320 400) or increased by the number of the local through crack interactions, which do not exist initially across the free crack faces.

The immediate state (positions and velocities) of the selected atoms has been saved every 25^{th} simulation step in all tests. The location of these selected atoms is shown in fig. 2. The state of the whole atomic system was saved when the simulations finished.

The calculations were done on 50 CPUs of the CESNET METACentrum clusters KONOS, MINOS, SKIRIT and SKURUT (the implementation of one simulation step intervened between 21 and 55 seconds depending on a machine performance).

3. Results and discussion

All tests (see tab. 1) were performed both for a perfect crystal and for a crystal with the embedded crack. The behavior differences are demonstrated in fig. 4. There is displayed the kinetic and potential energy for the test ③. Smaller changes are evident in both energies after the reflection from back side of crystal (time step $\approx 2\,100$) for the case of a sample with a crack (fig. 4 – bottom) in comparison with the perfect sample (fig. 4 – top). The reasons consist in the energy needed to passing the crack (time step $\approx 1\,050$).

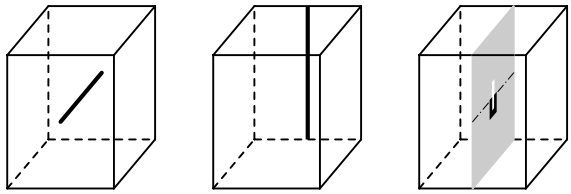

Fig. 3. The location of the atoms used in the following figures

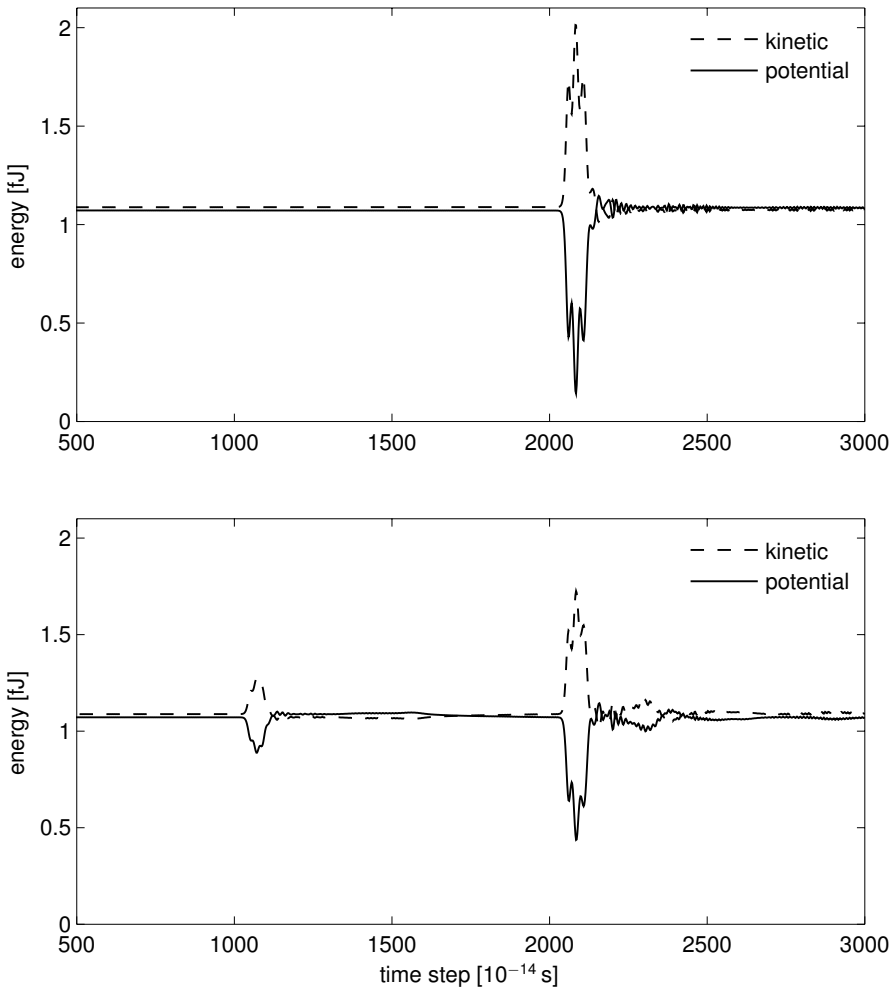

Fig. 4. The kinetic and the potential energy of the whole system for the test ③. The perfect crystal – top, the crystal with a crack – bottom

The influence of the pulse width on stress wave propagation for the sample with the crack is demonstrated in fig. 5. The absolute atomic velocity waveform on the y axis (see fig. 3 – left) at the time step 2150 (shortly after the back side reflection) for the test ① and ② is depicted in

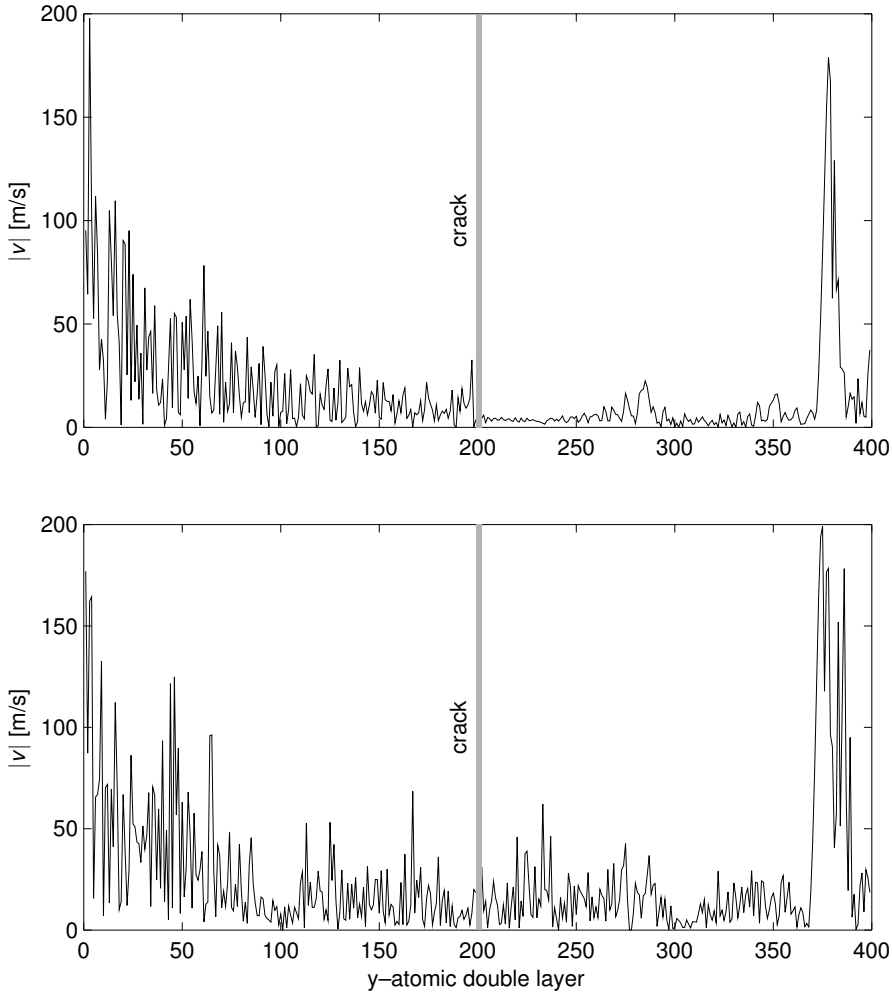

Fig. 5. The velocity magnitudes of the atoms on the y axis for the tests ① (top) and ② (bottom)

fig. 5. The pulse width for the test ① was 200 fs (top) and for the test ② was 400 fs (bottom). The location of the crack is denoted in these figures by means of the gray line.

Note the differences of the behavior for the test ① (narrow pulse) in the comparison with the test ② (wide pulse):

1. higher values of $|v|$ in neighborhood of the crystal front side,
2. latter reflection from the crystal back side and lower values of $|v|$ in its neighborhood,
3. lower values of $|v|$ in the area behind the crack.

Reasons consist in the local atomic interactions across the free crack faces that were monitored only for the test ②.

In the following figures, we are concentrated only on the tests, where the local atomic interactions across the free crack were detected, i.e. test ④, ②, and ⑤. Time progress of the global

kinetic and potential energies in the whole system together with the number of the local atomic interactions across the free crack is shown in fig. 6, fig. 10 and fig. 14. In these figures, the significant times from t_1 up to t_4 and u_1 up to u_4 are marked.

The pressure wave front reaches the crack plane at the time step t_1. The stress wave passes the crack at the time step t_2. The atomic absolute velocity waveform on the y axis (fig. 3 – left) is depicted for the time steps t_1 and t_2 in the fig. 7, fig. 11 and fig. 15 for the tests ④, ②, and ⑤, respectively. The location of the crack is again denoted in these figures by means of the gray line.

The time t_3 and t_4 denoted the moment closely before and after the reflection of the stress waves from the crystal back side, respectively. The situation at the atoms located on the perpendicular back face axis (see fig. 3–center) is illustrated for the time steps t_3 and t_4 in the fig. 8, fig. 12 and fig. 16 for the tests ④, ②, and ⑤, respectively.

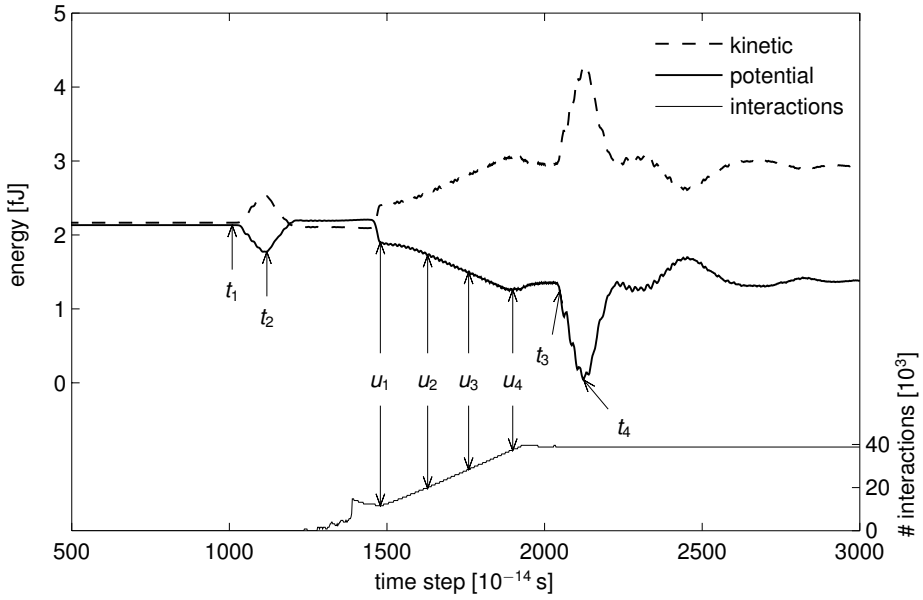

Fig. 6. The energies of the whole system and the number of the crack interactions for the test ④

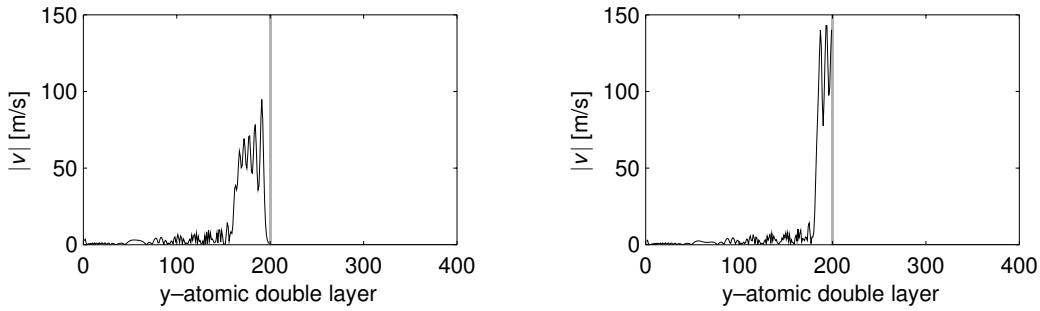

Fig. 7. The velocity magnitudes of the atoms on the y axis for the test ④, time t_1 – left, t_2 – right

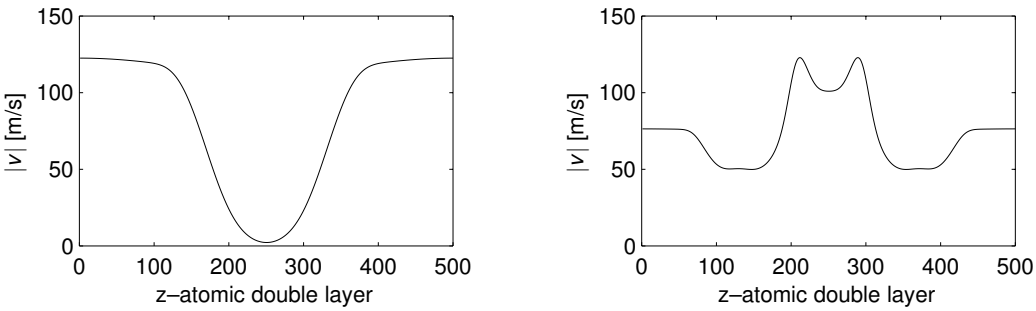

Fig. 8. The velocity magnitudes of the atoms on the z axis for the test ④, time t_3 – left, t_4 – right

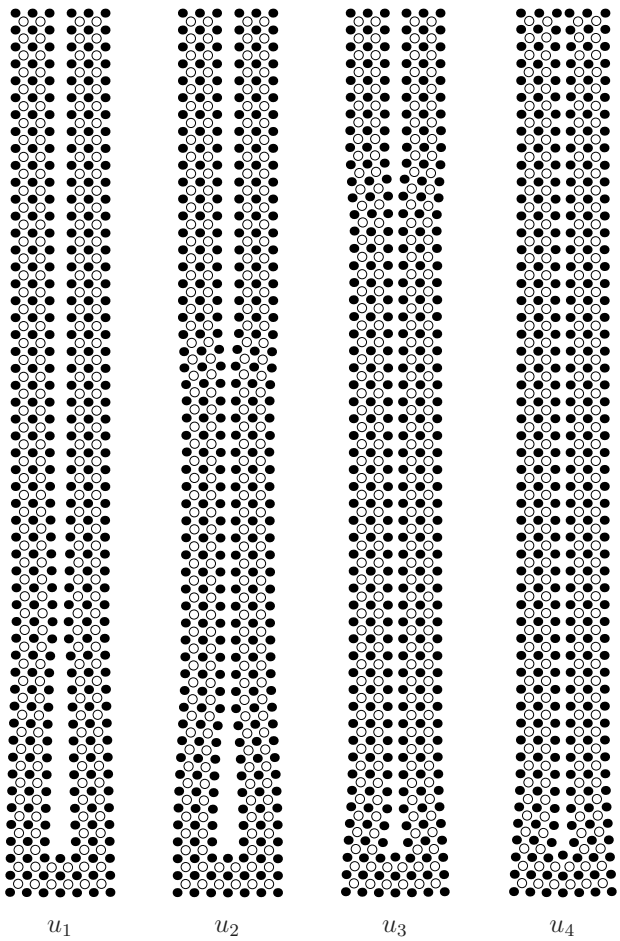

Fig. 9. The atom location in the crack neighborhood for the test ④ at the times u_1–u_4

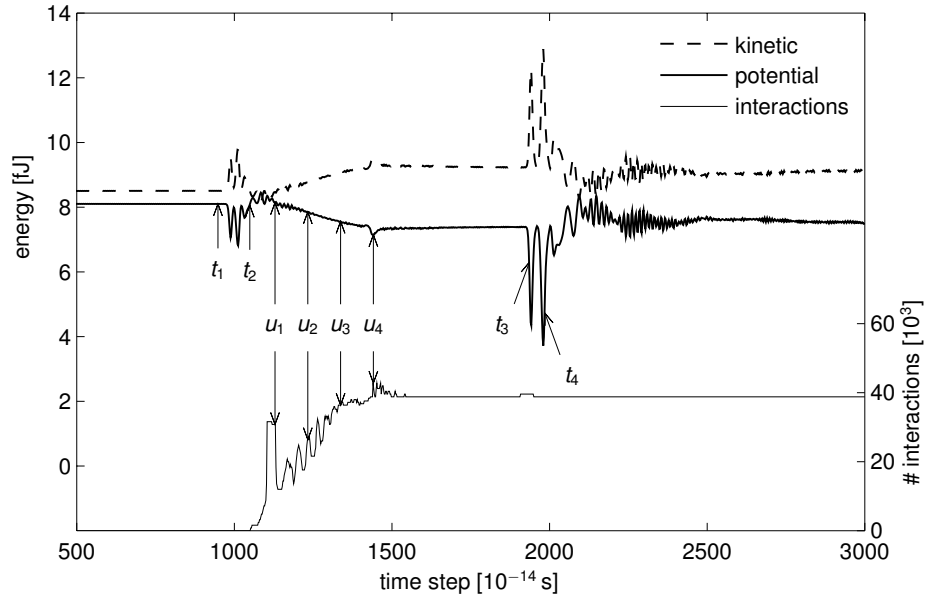

Fig. 10. The energies of the whole system and the number of the crack interactions for the test ②

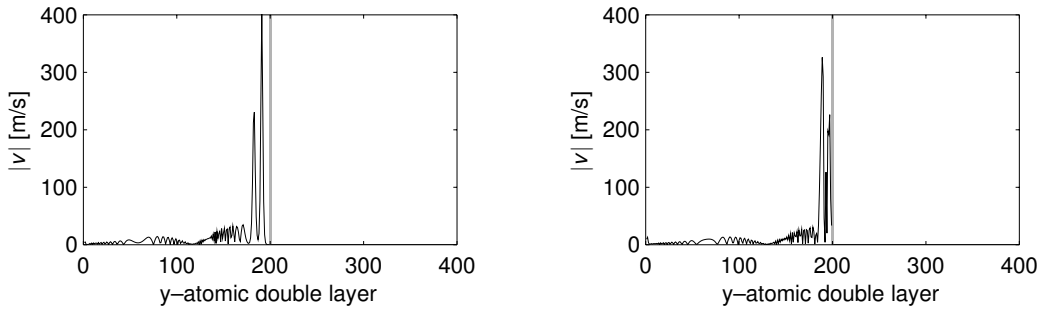

Fig. 11. The velocity magnitudes of the atoms on the y axis for the test ②, time t_1 – left, t_2 – right

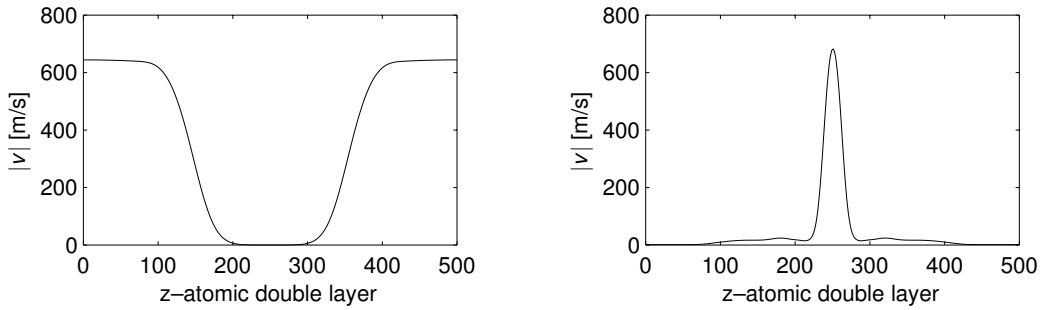

Fig. 12. The velocity magnitudes of the atoms on the z axis for the test ②, time t_3 – left, t_4 – right

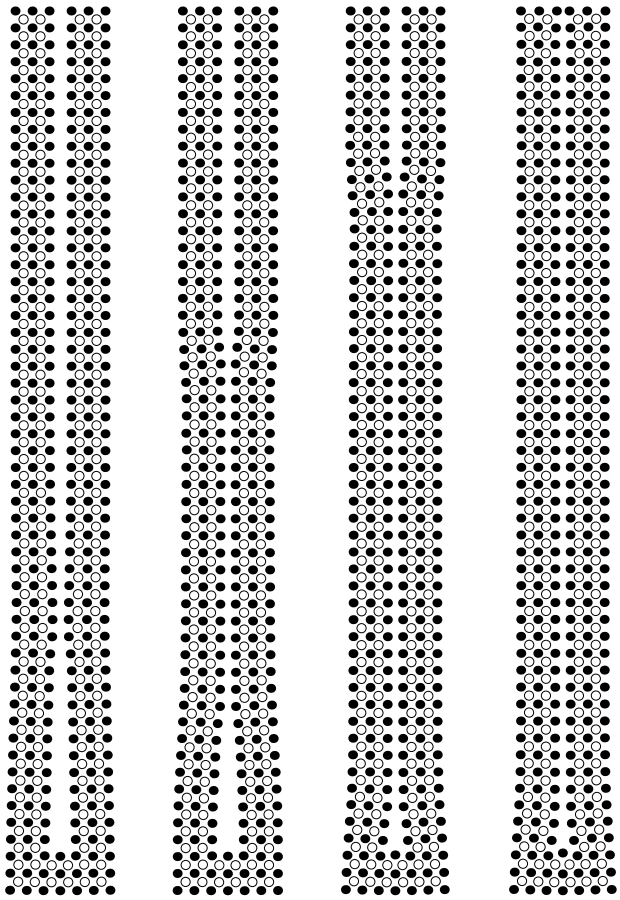

Fig. 13. The atom location in the crack neighborhood for the test ② at the times u_1–u_4

The atom location in the crack neighborhood (see fig. 3 – right) at the times u_1–u_4 for the test ④, ②, and ⑤, is shown in fig. 9, fig. 13, and fig. 17, respectively. Note that the numbers on horizontal axes in figs. 5, 7, 8, 11, 12, 15 and 16 denote atomic double layers (a_0).

The results of the test ④ are presented in fig. 6–9. The excitation pulse was pure compression for a period of 1 600 fs with a level of an applied stress 2.7 GPa in this test.

The kinetic and potential energy of the whole system as well as the number of the local atomic crack interactions is shown in fig. 6. There are sudden changes of the energies at the time moments t_1–t_4. These changes are caused by a reaching and passing the crack plane by the stress wave at the time steps t_1 and t_2, respectively. The changes of the energies at the time steps t_3 and t_4 are caused by the incidence and the reflection of stress waves from the crystal back side.

The times u_1–u_4 in fig. 6 denote some of the moments in which the number of the local atomic interactions across the free crack increases. The location of the atoms in the neighborhood of the bottom half of the crack (see fig. 3 – right) in these time moments is displayed in fig. 9. You can see the atoms are being gripped in the crack center in this case.

The results of the test ② are presented in fig. 10–13. The excitation pulse was pure compression for a period of 400 fs with a level of an applied stress 10.8 GPa in this test.

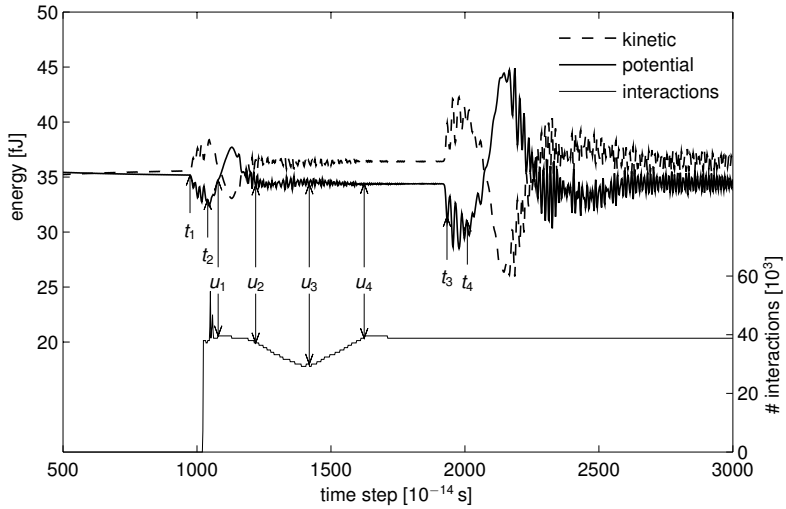

Fig. 14. The energies of the whole system and the number of the crack interactions for the test ⑤

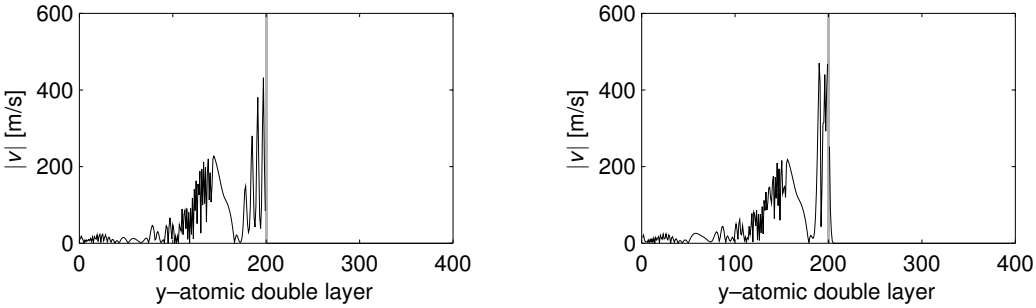

Fig. 15. The velocity magnitudes of the atoms on the y axis for the test ⑤, time t_1 – left, t_2 – right

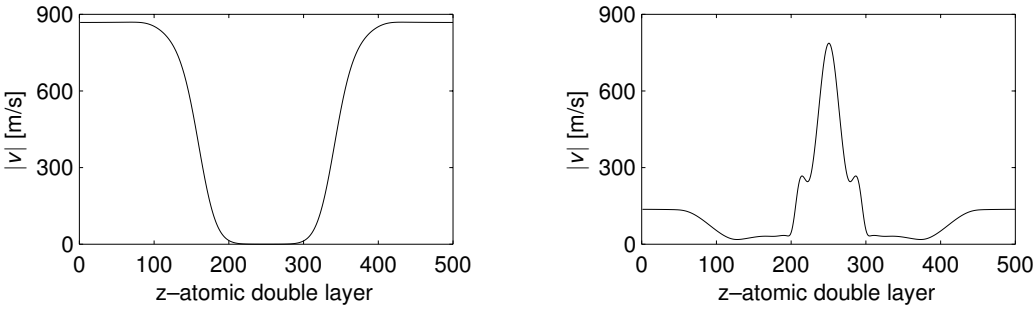

Fig. 16. The velocity magnitudes of the atoms on the z axis for the test ⑤, time t_3 – left, t_4 – right

Fig. 10 shows the kinetic and the potential energy of the whole system and the number of the local atomic crack interactions as in the previous case. The waveforms of the energies are not so smooth as in the previous case because of the four times larger applied stress. The time moments t_1 and t_2 correspond to the reaching and the passing the crack plane by the stress wave and the time steps t_3 and t_4 indicate the incidence and the reflection of the stress waves from the crystal back side.

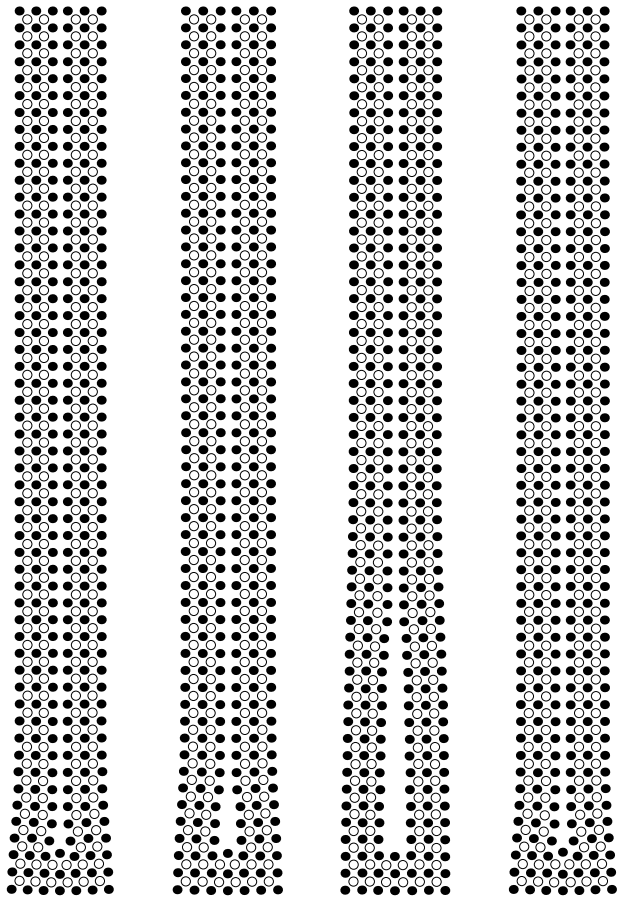

Fig. 17. The atom location in the crack neighborhood for the test ⑤ at the times u_1–u_4

The times u_1–u_4 in fig. 10 denote again some of the moments in which the number of the local atomic interactions across the free crack changes. The location of the atoms in the neighborhood of the bottom half of the crack (see fig. 3 – right) in these time moments is displayed in fig. 13. In this case the atoms are not being gripped in the crack center but rather closer to the crack front.

The presentation of the test ⑤ is in fig. 14–17. The excitation pulse was initially pure compression for a period of 800 fs and subsequently pure tension for a period of 800 fs. The level of applied stress was 10.8 GPa as in previous test.

The kinetic and the potential energy waveforms of the whole system and the number of the local atomic crack interactions are displayed in fig. 14. The notation of the time moments t_1–t_4 has the same sense as in the two previous cases.

Fig. 17 is very interesting. The crack is nearly gripped at the time u_1, then it starts to open at the crack front. The local minimum of the local atomic crack interaction number has occurred at the moment u_3 (see fig. 14). At this time the crack is most opened and it is gripped again at the time step u_4.

Note that all simulations was performed twice to see reproducibility of the results.

4. Summary

This paper presents the results of our research on propagation of a pressure stress waves in a bcc iron crystals with the basic cubic orientation. The simulations are based on molecular dynamic method and utilized an N-body potential of a Finnis-Sinclair type for a transition metals, [2, 3].

The comparison of the perfect crystal and the crystal with embedded crack is mentioned here. A pre-existing Griffith (through) crack is considered, where the local atomic interactions across the free crack faces do not exist initially. The influence of the shape, width and amplitude (stress level) of the excitation pulse is studied. We observed the behavior differences of atoms in the crack neighborhood caused by activation of the local atomic interactions across the free crack faces, which is very important result for further analysis. The most successful pulses for transfer of the energy across crack faces are the pulses denoted in tab. 1 by ④ and ②. In these two cases we detected changes in the local kinetic energies of individual surface atoms on both opposite and front crystal surfaces caused by the activation of the local atomic interactions across the initially free crack faces. It will be further analyzed. According to author's knowledge, all the presented new results are not published till now.

Our future research will be oriented to investigations of a stress wave propagation after the critical interaction crack-pressure pulse and on a possible mapping of the internal cracks in materials via this non-linear phenomenon on crystal surfaces by analyzing of the atomic displacements and velocities of surface atoms, which can bring useful information for the detection of defects by the displacement or velocity sensitive transducers in NDT.

Acknowledgements

This work was supported by the Czech Science Foundation under the grant 101/07/0789 and the research project AV0Z20760514 of AS CR. The access to the METACentrum clusters provided under the research intent MSM6383917201 is highly appreciated.

References

[1] F. F. Abraham, R. Walkup, H. J. Gao, J. M. Duchaineau, T. D. D. L. Rubia, M. Seager, Simulating materials failure by using up to one billion atoms and the world's fastest computer. Workhardening, P. Natl. Acad. Sci. USA, 99 (2002) 5 783–5 787.

[2] G. J. Ackland, et al., Computer simulation of point defect properties in dilute Fe-Cu alloy using a many-body interatomic potential, Phil. Mag. A 75 (1997) 713–732.

[3] M. W. Finnis, J. E. Sinclair, A simple empirical N-body potential for transiton metals, Phil. Mag. A 50 (1984) 45–55.

[4] Y. F. Guo, C. Y. Wang, D. L. Zhao, Atomistic simulation of crack cleavage and blunting in bcc Fe. Materials Sci. Eng. A 349 (2003) 29–35.

[5] A. Latapie, D. Farkas, Molecular dynamics simulations of stress induced phase transformation and grain nucleation at crack tips in Fe. Modelling Simul. Mater. Sci. Eng. 11 (2003) 745–755.

[6] K. Nishimura, N. Miyazaki, Molecular dynamic simulation on plastic deformation processes around a crack tip under cyclic loading. ICF XI, Turin, March 20–25, 2005.

[7] P. Pacheco, Parallel Programming With MPI, Morgan Kaufmann, 1996.

[8] V. Pelikán, P. Hora, A. Machová, Wave propagation simulations by molecular dynamics methods, (in Czech), Proceedings of the 21st Conference Computational mechanics 2005, pp. 463–470.

[9] V. Pelikán, P. Hora, A. Machová, Wave propagation simulations in copper and nickel crystals, (in Czech), Proceedings of the 22nd Conference Computational mechanics 2006, pp. 453–460.

[10] V. Pelikán, P. Hora, A. Machová, O. Červená, The simulation of a wave propagation in a bcc iron crystal with a crack, Applied and Computational Mechanics 1 (1) (2007), 225–232.